25th ABCM International Congress of Mechanical Engineering
October 20-25, 2019, Uberlândia, MG, Brazil

COB-2019-0895
LIMIT OF USING COMPUTED TORQUE CONTROL OF AUTONOMOUS AIRSHIPS IN WIND ENVIRONMENT

Constantino G. Ribeiro
CEFET-RJ, UnED Itaguaí, Rodovia Mário Covas, lote J2, quadra J – CEP: 23810-000, Distrito Industrial de Itaguaí – RJ – Brasil
constantino.g.ribeiro@gmail.com, constantino.ribeiro@cefet-rj.br

Luciano Santos Constantin Raptopoulos
CEFET-RJ UnED Nova Iguaçu, Estrada de Adrianópolis, 1317, - CEP: 26041-271 - Nova Iguaçu – RJ – Brasil
luciano.raptopoulos@cefet-rj.br

Max Suell Dutra
COPPE - UFRJ, Centro de Tecnologia, bloco G, salas 202 / 203 / 204, Universidade Fede-ral do Rio de Janeiro, Cidade Universitária - Ilha do Fundão, Caixa Postal 68.503, CEP 21945-970, Rio de Janeiro – Brasil
max@mecanica.coppe.ufrj.br

Abstract. *The studies of the swarm of UAVs (Unmanned Aerial Vehicles) have increased, and they are part of many daily tasks. There are several proposals for aircraft that operate autonomously, each with its advantages and disadvantages. An interesting proposal, with a reasonable cost-benefit ratio, is the use of autonomous dirigibles. One of the disadvantages of the airship is its sensitivity to strong wind environments. The proposed work studies the limit of using autonomous airships controlled by computed torque method in a strong winds' environment. The study established a threshold of wind speed to an autonomous airship be controlled by computed torque method. The use of simulations with wind conditions will showed the limit of computed torque control by data like error to reach the path, variation on absolute speed, effort to control the UAV, and others. These data will help to improve the control system proposed.*

Keywords: *Computed torque control, strong winds, UAV, airships*

1. INTRODUCTION

The use of airships in various long-term tasks can be found in (Polmar, N. June 2011) and (Machry, C. R. 2003). The popularization of other types of aircraft both fixed wing (aircraft and gliders) as well as those of rotating wings (helicopters) especially after the second great war can be attributed to the significant evolution of materials sciences, mechanical (and aeronautics) as well and control methods and a new type of aircraft - remotely controlled, started to be used, without pilots avoiding losses of life in some missions.

The use of unmanned aerial vehicles (UAVs) added new costs to operations, like ground control stations and more skilled personnel in these operating facilities. One way to decrease these high costs is making these UAVs less human dependent, increasing their autonomy with less remote-control stations' dependence. A way to do this is to embed the control systems in the UAV, taking consideration of operational characteristics of the aircraft used, as its interactions with the environment.

2. RELATED WORKS

The attitude control of a robotic airship that maintains a predetermined position is proposed in (Yang, J. W. 2012) where the slider technique is implemented through a system based on Fuzzy logic, using Lyapunov filter and the stabilization theorem, the which are developed and implemented.

The task of controlling a steerable robot in an environment subject to strong winds was studied by (Hitomu Saiki, T. 2010). The proposed solution was the use of control of the stability of the aircraft through the technique of following the route, sailing against the wind with the stability control being done by a control function (Lyapunov function) according to pre-established control rules. Satisfactory tests were performed with a suitably adapted 12-meter remote blimp.

A proposal to control the buoyancy and attitude of a dirigible using only a density variation of a pair of cuffs was proposed in (Xiaotao Wu, C. M. 2009). In this proposal the idea is to use the system present in several aquatic gliders as

the means of move of the aircraft but taking into account the difference in behavior of such structures in the atmosphere where air is a compressible fluid. To make the mechanism viable, a feedback control system is proposed from the equations of motion of the aircraft studied. In this control system a linear quadratic regulator is used to generate feedback gains.

In (Jörg Müller, N. K. 2011), a system for autonomous navigation of a mini airship for indoor surveillance is proposed. First a collision-free environment is generated from a route search algorithm of type A*, and in a second step, there is a planning tree that generates the possible optimal routes in 12-dimensional state space. This space is then reduced to one of four dimensions using a smaller Euclidean distance heuristic, which generates new routes based on planning trees and information obtained by a finite horizon function based on linear quadratic time. Tests were conducted in a real-world large environment consisting of two rooms.

A simple and robust application of a fuzzy logic navigation system is described in (P. González, WB. 2009). A commercial airship robot (Plantraco), with a 52 "rigid cave, was used as prototype. 200 grams of fillers. Ultrasonic sensors provide information about the environment and feed a fuzzy collision avoidance system that generates 180-degree swerves. The results of the tests demonstrated a balanced behavior of the fuzzy controller which can even be trained.

A route control system for a steerable robot used in the surveillance and monitoring of areas that have suffered natural disasters is the theme of (T. Fukao, AY. 2008) which uses the field velocity and an optimal reverse tracer controller as a control strategy. Such strategy was effective in environments with winds, as it avoids the use of time in the formulation of trajectories. The optimal inverse controller consists of a system of two coordinates (x and y), nonlinear looping based on a Hamilton-Jacobi-Bellman equation, and Lyapunov filter, for the horizontal control of the vehicle. The practical tests were carried out by a dirigible with 12,2 meters of length, admissible load of up to 15 kilograms, equipped with sensor of winds and camera stereo.

In (Axel Rottmann, C. P. 2007) a online reinforced learning method was used as route control. In this work the maintenance of the altitude of the airship without the previous knowledge of the environmental conditions. Through the use of agents (autonomous computer programs), which are given bonuses for correct actions maximizing the solution search method used (Monte Carlo method). This method allows a direct learning (without the necessity of previous storage) by the agents. To avoid problems related to the size of the search space relative to the learning function, a Gaussian function on the space of pairs of action states is used, where the states of these pairs are captured by ultrasonic sensors with a Kalman filter to the removal of noise during the movement of the airship. The practical tests were carried out with a commercial airship of 1.8 meters in length in a factory facility with vain of up to 5 meters in height.

In (José R. Azinheira, P. R. 2002) a camera is used to obtain images that, after proper modeling, generates a set of elementary signals, establishing a relationship between velocity and elements on land (target). The modeling is similar to the pendulum problem, but in this case, what is wanted is the association of movement at a distance equal to zero in relation to the airship. In this modeling the effects of winds and other environmental disturbances are also considered. Tests were conducted in three environmental situations: no wind and no disturbances; with winds and weak disturbances; and with strong winds and disturbances.

3. AN AUTONOMOUS AIRSHIP

As already mentioned, the use of dirigibles in long-term tasks has already proved its effectiveness in (Machry, C. R. 2003) and (Fossen, T. I., 1994). With the advent of UAVs and the need to reduce their costs, the of airships became more attractive due to their low fuel consumption, high autonomy, ease of use, and low environmental impact. However, some factors limit or restrict the use of airships: environments of strong winds can hinder the correct operation of this type of platform.

As described in (Fossen, T. I., 1994), (Fossen, T. I., 2002), and (Ribeiro, C. G. et al. 2015) the kinematics and dynamics of an airship and function of the system reference, their dimensions, and their total mass. In this study, the equations of the kinematics of an ellipsoid dirigible with 28 meters in length and 9 meters in width (Ribeiro, C. G. et al. 2017) were used. The airship kinematics and dynamics were developed using Newton-Euler definitions and according to an airship geometric arrangement (propellers localization and total mass). The solution of developed equations lead control input of torques and control forces for the proposed airship, and a control system suitable for the airship was developed.

3.1 Computed torque control

Computed torque control uses a control input to eliminate the non-linearity of dynamic modeling. This new input must have a parameter that will become the new control input of an equivalent dynamic linear system. An advantage of the computed torque is eliminating of the nonlinearities of the dynamic model, which is mathematically demonstrated by new inputs of the linearized system, obtaining a dynamic and stable response. Computed torque can be used in a mechanical system described by equation (1):

$$M(q)\ddot{q} + C(q,\dot{q})\dot{q} + G(q) = \tau \quad (1)$$

Where:

- *M(q)* is the inertia matrix of dimension *n* x *n*;
- $C(q,\dot{q})$ is the matrix of centrifugal and Coriolis forces of dimension *n* x *n*;
- *G(q)* is a vector of gravitational components of dimension *n* x *1*;
- *q* is a vector of positions of dimension *n* x *1*;
- τ is the vector of torque and forces of dimension *n* x *1* which causes the system to be fully actuated.

The system must be controlled in a steady state, through *u* so that q has the same value of *q* in the desired position with minimal or no error. In the computed torque a control signal *u* is generated to linearize the system and a second control signal *v* is used to fit mesh into the desired dynamics. To use this, the nonlinearities and the control input must be in the same equation, isolating $\ddot{q}$ in one side of the equation and so there is a new control input *v* (2) e (3):

$$v = \ddot{q} = M(\ddot{q})^{-1}[\tau - G(q) - C(q,\dot{q})\dot{q}] \quad (2)$$

Or

$$\tau = M(q)v + G(q) + C(q,\dot{q})\dot{q} \quad (3)$$

Part of the signal τ cancels the output of system nonlinearities. Once the system control law has been determined, a linear control strategy is applied to determine v. If the desired trajectory $q_{desired}(t)$ is selected it will be guaranteed by an exit or follow-up error defined as (4):

$$e(t) = q_d(t) - q(t) \quad (4)$$

Where the influence of the input data of τ on the output error can be noticed when the expression (4) differs twice:

$$\dot{e} = \dot{q}_d - \dot{q} \quad (5)$$

Or

$$\ddot{e} = \ddot{q}_d - \ddot{q} \quad (6)$$

Solving equation (6) in $\ddot{q}$ and substituting in the equation (3) there is a new equation (7):

$$\ddot{e} = \ddot{q}_d + M^{-1}(N + \tau_d - \tau) \quad (7)$$

Equation (7) can be used to define a function for the control input (8): $u = \ddot{q}_d + M^{-1}(N - \tau)$ (8)

And a disturbance function (9): $\omega = M^{-1}\tau_d$ (9)

4. WIND DISTURBANCE

The wind is a critical external disturbance in an airship control system. The airship is a light them air aircraft, so windy environment is more demanding for control issues. This work uses the projection of wind direction into cartesian axis (*x*, *y*, *z*) of inertial reference to compute the extra airship drag to be used in control system of the blimp, as shown in Fig. 1.

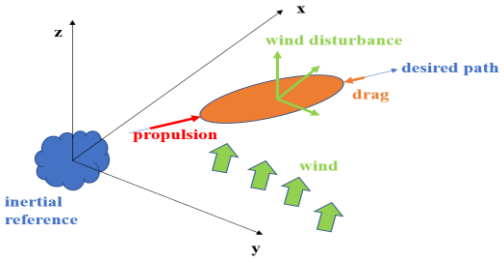

Figure 1 - Wind effect over control system.

Each cartesian projection of wind direction is used into equation (1) as an external disturbance, so wind influence in the efforts to keep the airship into a path is computed as shown in Fig. 2.

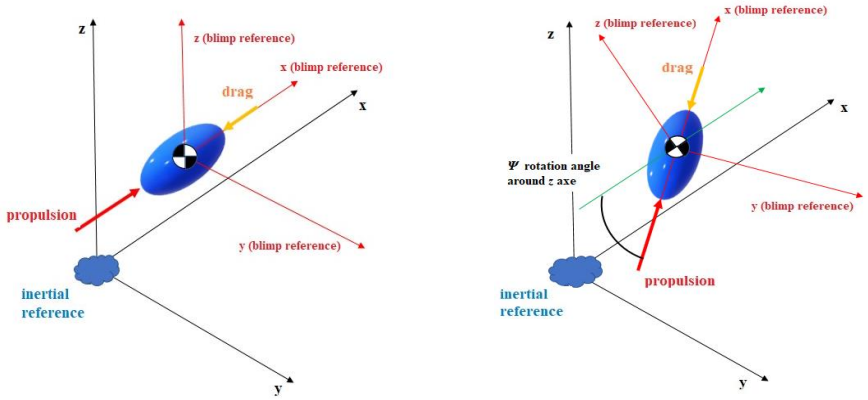

Figure 2 – Wind effect in new blimp orientation.

In most cases, occurrences of up or down winds are not common. Thus, in this work, only the winds in the *xy* plane of the inertial frame were computed, that is, without the *z* component. The introduction of a vector in *z* and simple and its use is similar to the approach adopted below: projection of the force generated by the wind in the axes x and *y*.

As an example, the situation that occurs in Fig. 3, the left side where the wind falls on the dirigible at an angle of 135 degrees (trigonometric circle) from right to the left at the beginning of its journey (according to inertial orientation). In the next moment, in Fig. 3, the airship changes course and the incidence of the wind changes.

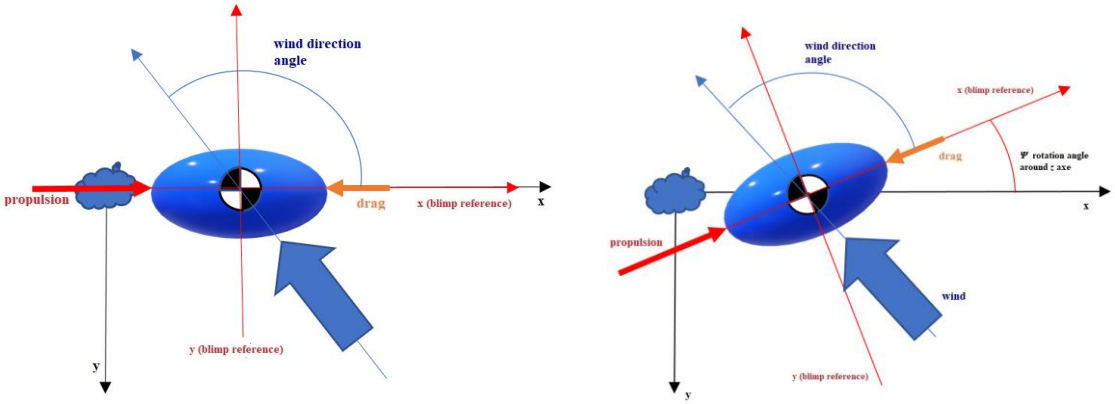

Figure 3 – New wind projection.

Making the free-body diagram of the forces acting on the x-axe and y-axe, instant A of Figure 3, we have the following forces acting on this plane as shown in Fig. 4.

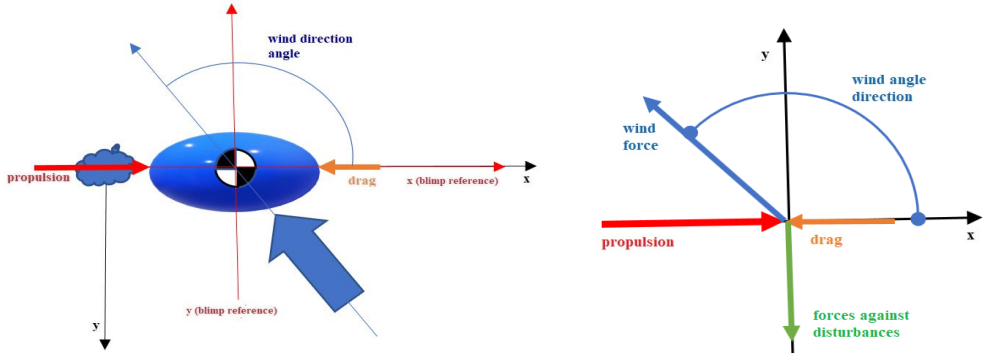

Figure 4 – Forces diagram.

In a second analysis, making the free-body diagram of the forces acting on the axes *x* and *y*, in Fig. 3 on the right, we have the following forces acting on this plane as shown in Fig. 5 on the left. In this new moment, it is noticed that although the direction of wind remains the same, the rotation angle ψ around the angle *z*, generated a new angle of action of the wind force due to the new relative position of the airship in relation to inertial frame as shown in Fig. 5 on the right.

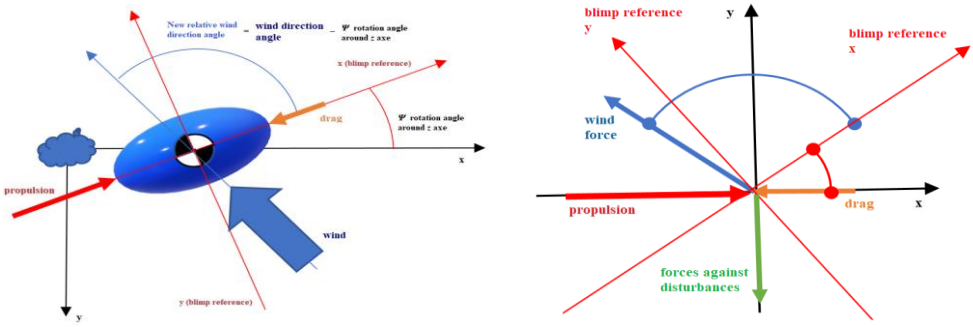

Figure 5 – New forces diagram.

Making the free-body diagram and the sum of forces in the x and y axes, we will have:
Right of Fig. 4:

$$\sum Forces\ in\ x\ axel = 0 \qquad \text{propulsion . cos}(\psi) = \text{wind force . cos (wind angle)} + \text{drag force;} \tag{10}$$

$$\sum Forces\ in\ y\ axel = 0 \qquad \text{wind force . sin (wind angle)} = \text{force against disturbance;} \tag{11}$$

Right of Fig. 5:

$$\sum Forces\ in\ x\ axel = 0 \qquad \text{propulsion . cos}(\psi) = \text{wind force . cos (wind angle)} + \text{drag force . cos }(\psi); \tag{12}$$

$$\sum Forces\ in\ y\ axel = 0 \qquad \text{propulsion . sin}(\psi) + \text{wind force . sin (wind angle)} = \text{drag force . sin }(\psi) + \text{force against disturbance;} \tag{13}$$

The new free-body diagram can be shown in Fig. 6.

Figure 6 – New free-body diagram.

New orientation axes of the forces acting on the airship according to the rotation of these same axes of the angle ψ (rotation about the *z* axis). This angle ψ will be added to the angle of the wind blowing direction and this sum of angles will be used in MatLab© simulation equations.

New values of the angle of incidence of the winds on the airship will depend on the value of the angle ψ of rotation of the airship around its own *z* axis in its center of gravity, being able to diminish or increase its value according to the trajectory of the airship and its orientation, always obeying the trigonometric and Cartesian rules. The equations (12)

and (13) are incorporated into the system developed in MatLab© simulation environment for airship operation and its control plant as described in the next section.

5. CONTROL SYSTEM

The airship control system was developed in MatLab© environment. It was based on kinematics and dynamics of an ellipsoid shape airship with 28 meters of length and 7 meters wide with a payload of 1000 kilograms force (C. G. Ribeiro et al. 2017). The contour variables used were: airship cruiser speed of 33,33 meters per second (120 km/h); 2000 kilograms force of a total payload for airship envelop, climbing tax of 0,001 meters per second; and maximal turn speed around z-axis of 0,35 radians per second. A MatLab© control system scheme is shown in Fig. 7.

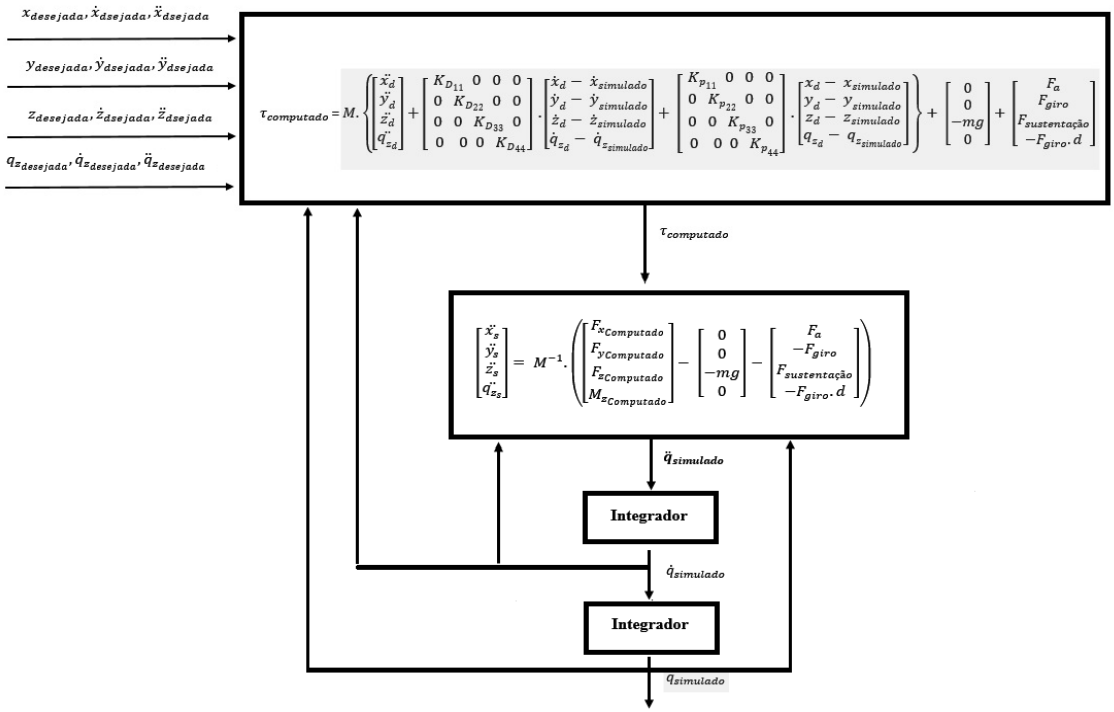

Figure 7 – MatLab© proposed control system.

6. TESTS AND RESULTS

The tests established a limit to use airships controlled by our computed torque in windy environments. The simulations were performed in a MatLab© environment described by Fig. 7, with data values described in (C. G. Ribeiro et al. 2017) in section 5 and with wind behavior described in Fig. 2. The desired trajectory is an upward spiral. Wind values from zero to 90 km / h (5 km / h increments) were used for an incidence angle of 135 degrees according to the trigonometric circle.

The results obtained were organized into three graphs: i) A graph with error results in meters in the *x* direction resulting from the wind forces applied to the airship, Fig. ii) A graph with error results in meters in the *y* direction resulting from the wind forces applied to the airship, Fig. 9; and iii) A graph with results of the variations in the absolute speed of the airship resulting from the forces of the winds applied to the airship, Fig 10.

Fig. 8 describes a small and acceptable variation of the x-coordinates for the winds acting on the airship during all applied values.

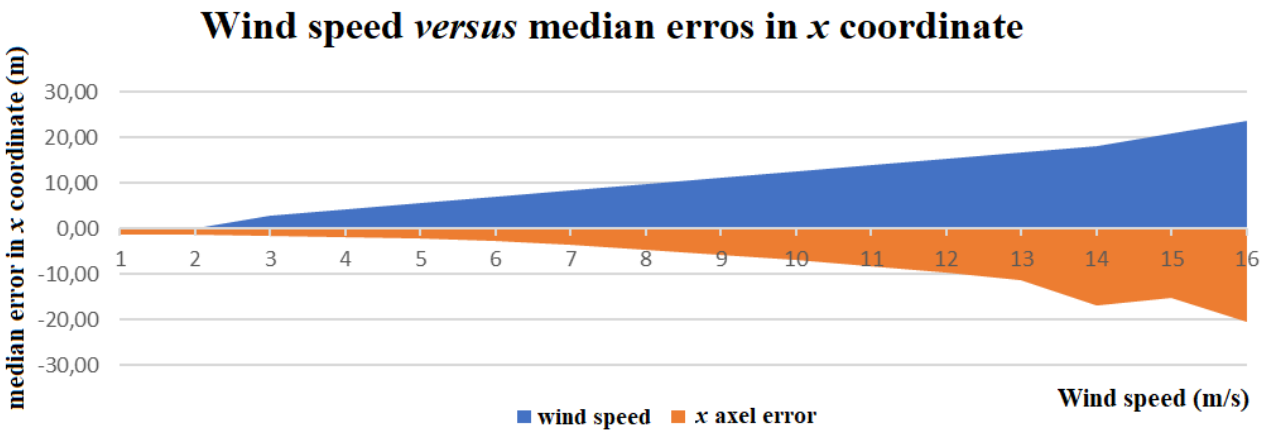

Figure 8 – Speed of wind *versus* erros in *x* axel.

Fig. 8 describes the variations of the coordinates in *y* for the winds that act in the dirigible. It is noted that from a speed of 65 km/h on, the variation of errors in the *y* coordinate is much larger and significant than the values of the errors in the *x* coordinate.

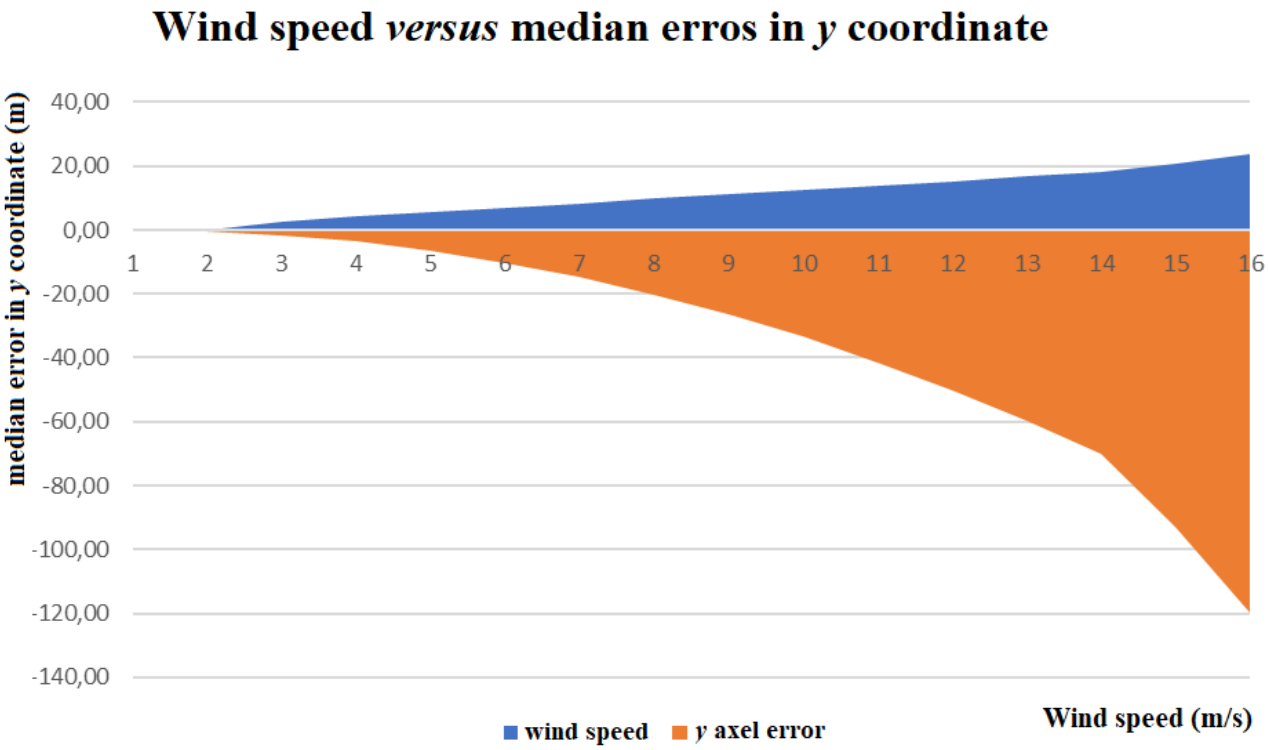

Figure 9 - Speed of wind *versus* erros int *y* axel.

Fig. 10 describes the variations of the absolute median velocities for the winds that act in the dirigible. Very small values of these variations are noted although from the speed of 65 km/h the speed oscillates predictably around the median speed well near the desired absolute velocity.

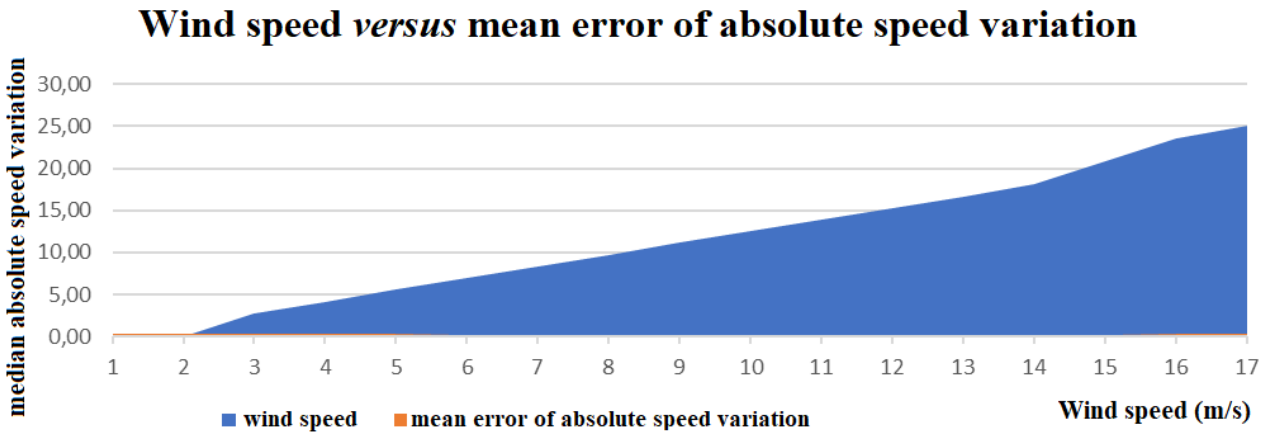

Figure 10 – Absolute median speed *versus* speed of wind.

7. CONCLUSIONS

The objective of this work, to determine the speed limit for the use of the proposed airship using a computed torque control system was reached. The wind speed limit was set at 65 km/h, due to the increasing behavior of the errors in the coordinate *y* from this speed. So, at the beginning of tests Fig. 11 shows trajectory to be followed, and Fig. 12 shows the errors in the absolute velocity, for a no wind situation.

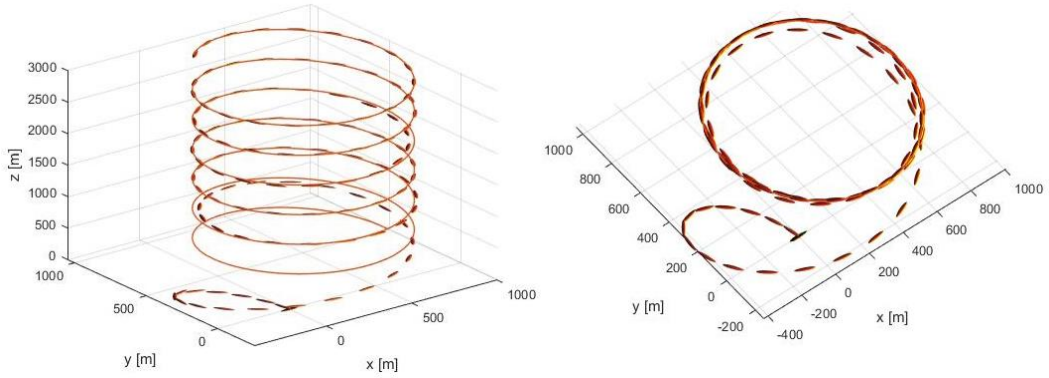

Figure 11 – Following the desire path with no wind.

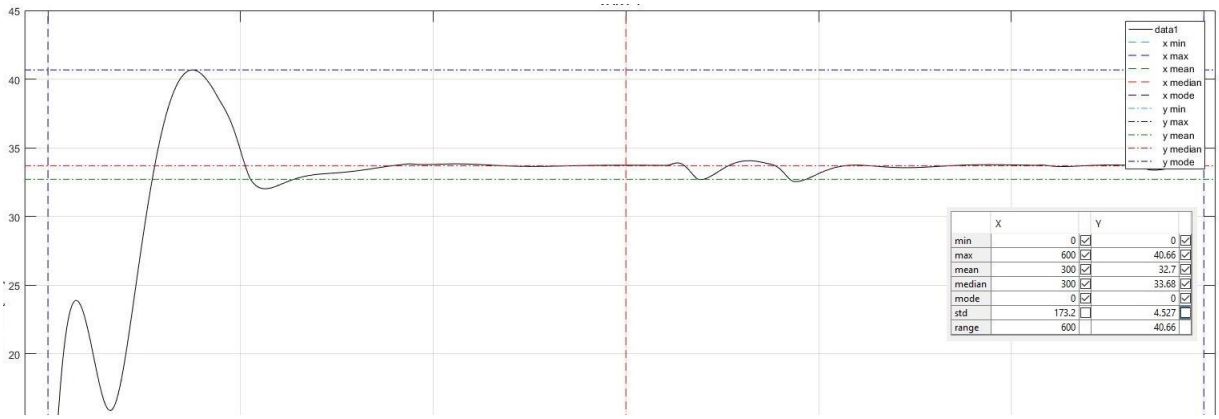

Figure 12 – Absolute speed with no wind.

The wind speed limit was set at 65 km/h, due to the increasing behavior of the errors in the coordinate *y* from this speed. From 65 km/h the winds begin to induce considerable errors in the direction followed by the dirigible, especially in the coordinate *y*, as shown in Fig. 13. As shown by Fig. 8 and Fig. 9 there is a large difference between the values of errors in the *x*-coordinate axis (smaller values) and errors in the *y*-coordinate axis (smaller values). This is because the

airship is an under-operated vehicle (CG Ribeiro et al., 2017) and there are no actuators in the direction of the *y* coordinate, which requires a combined control of the other actuators in the control of the route in this direction which gives a greater error and greater sensitivity to external perturbations in this direction.

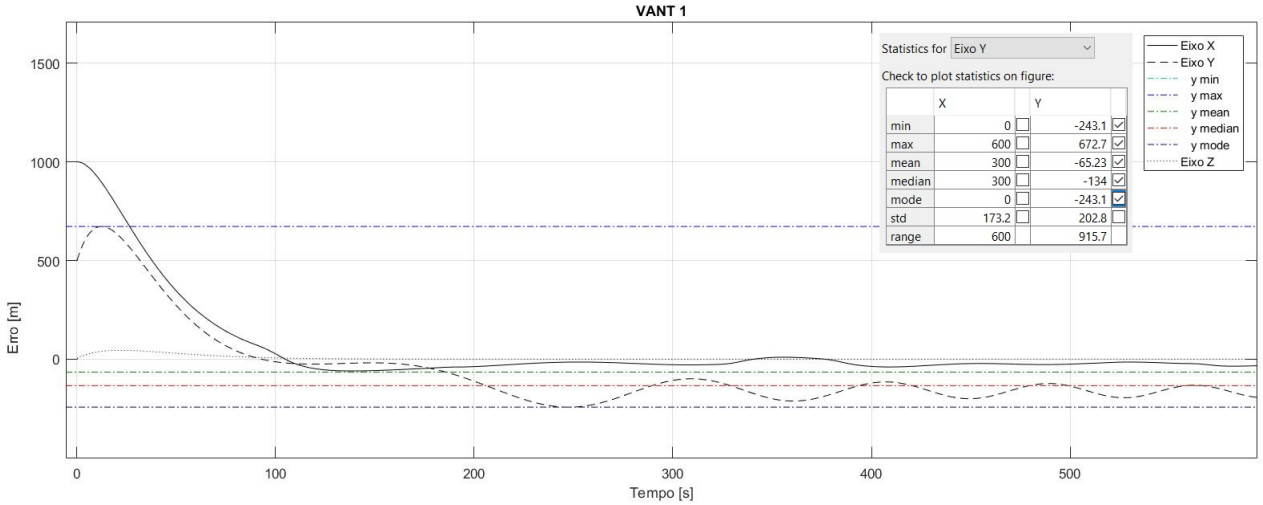

Figure 13 – Erros of: *x*, *y* and *z* axel under wind (65 km/h).

From 65 km/h the winds begin to distort the speed and it does not remain stable although the median speed is within acceptable values (maximum error: 0,33666 m/s or 1.0099%), with peaks of 29 m/s and 37 m/s, Fig. 14. This large variation may render applications unviable (aerial photogrammetry, geophysical data collection, etc.) where constant velocity is essential.

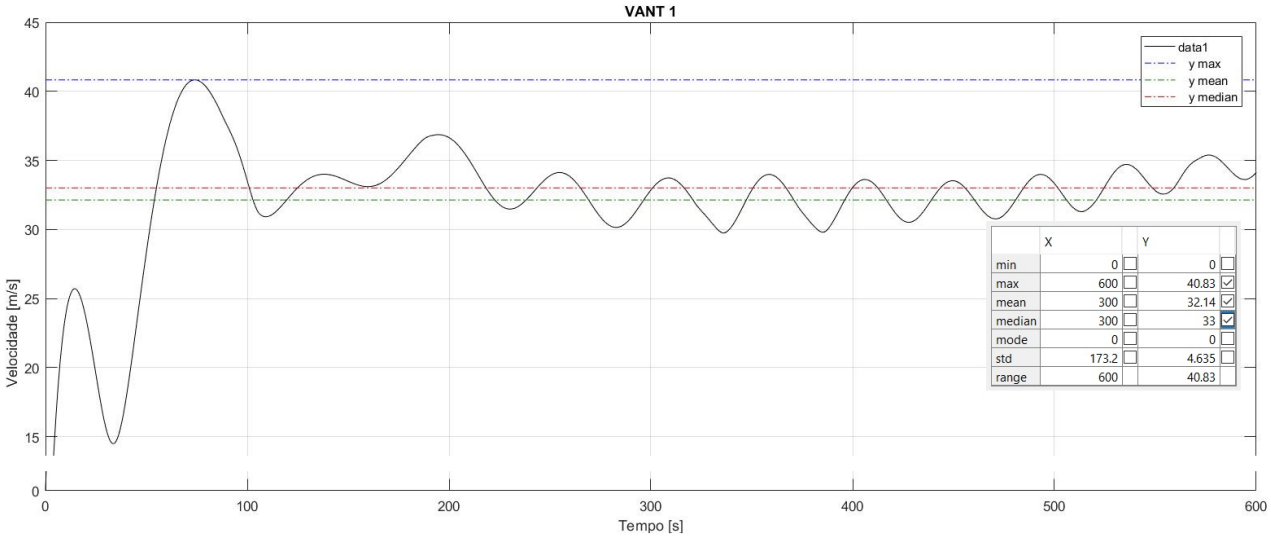

Figure 14 – Absolute speed variation under winds.

Finally, the trajectory cannot be maintained, within acceptable errors, with winds above 65 km/h, Fig. 15. In addition, Fig. 15 shows the greatest sensitivity and major errors in the *y*-coordinates when strong winds act on the airship.

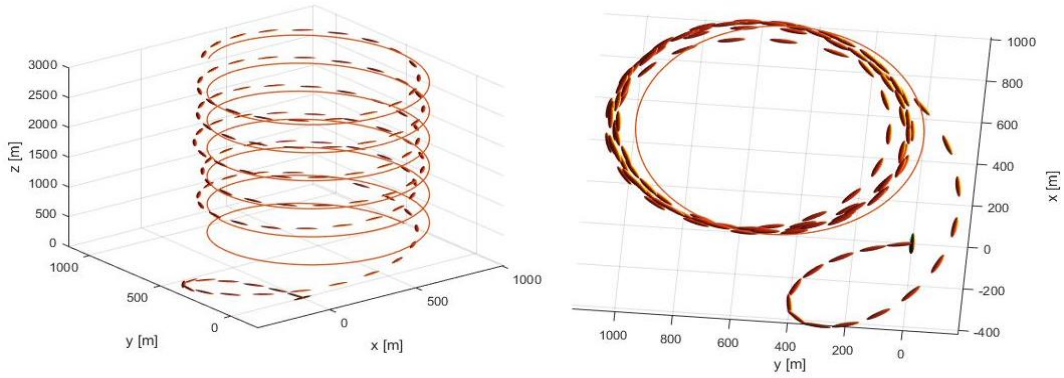

Figure 15 – Blimp path under strong winds

8. ACKNOWLEDGEMENTS

This work is sponsored by National Council of Scientific and Technologic Development (Conselho Nacional de Desenvolvimento Científico e Tecnológico - CNPq) and (Centro Federal de Educação Tecnológica Celso Suckow da Fonseca – CEFET/RJ).

9. REFERENCES

Axel Rottmann, C. P. October 29 to November 2 2007. "Autonomous Blimp Control using Model-free Reinforcement Learning in a Continuous State and Action Space". *Proceeding of International Conference on Intelligent Robots and Systems*, 2007. IROS 2007, pp. 1895-1900.

Fossen, T. I., 1994. "Guidance and Control of Ocean Vehicles", John Wiley & Sons, West Susses, England.

Fossen, T. I., 2002. "Marine Control Systems, Guidance, Navigation, AND Control of Ships, Rigs and Underwater Vehicles", ISBN 82-92356-00-2, Marine Cybernetics, Trondheim, Norway.

Hitomu Saiki, T. F. 8-10 September 2010. "Hovering Control of Outdoor Blimp Robots Based on Path Following". *2010 IEEE International Conference on Control Applications (CCA)*.

Jörg Müller, N. K. 25-30 September 2011. "Autonomous miniature blimp navigation with online motion planning and re-planning". *In proceeding of 2011 IEEE/RSJ International Conference on Intelligent Robots and Systems*, IROS 2011.

José R. Azinheira, P. R. May 2002. "Visual Servo Control for the Hovering of an Outdoor Robotic Airship". *Proceedings of the 2002 IEEE International Conference on Robotics & Automation*, Washington, DC.

Machry, C. R. 2003. "As Potencialidades de Emprego dos Dirigíveis no Transporte de Carga". Reista da UNIFA.

P. González, W. B. January 2009. "Developing a Low-Cost Autonomous Indoor Blimp". *Journal of Physical Agents*, pp. VOL. 3, NO. 1.

Polmar, N. June 2011. "Ships That are Liter Than Air". Acesso em 22 de 1 de 2013, disponível em USNI - U. S. Navy Institute: http://www.usni.org/magazines/navalhistory/2011-05/ships-were-lighter-air.

Ribeiro, C. G., et al. 2015. "A Robotic Flying Crane Controlled by an Embedded Computer Cluster", *in proceeding of XII LARS – Latin American Robotics Symposiun* 2015 - 978-1-4673-7129-2/15 - 2015 IEEE DOI 10.1109/LARS-SBR.2015.

Ribeiro, C. G.,; Raptopoulos, L. C., Dutra, M. S. "A platform for autonomous path control of unmanned airship". *Journal of the Brazilian Society of Mechanical Sciences and Engineering*. , v.5, p.1 - 13, 2017.

T. Fukao, A. Y. 6-11 July 2008. "Inverse Optimal Velocity Field Control of an Outdoor Blimp Robot". *Proceedings of the 17th World Congress The International Federation of Automatic Control*, Seoul, Korea.

Xiaotao Wu, C. M. 27-29 August 2009. "Modelling and linear control of a buoyancy-driven airship". *Proceeding of 7th Asian Control Conference, 2009*. ASCC 2009.

Yueneng Yang, J. W. April 2012. "Adaptive fuzzy sliding mode control for robotic airship with model uncertainty and external disturbance". *Journal of Systems Engineering and Electronics* Vol. 23, No. 2.

10. RESPONSIBILITY NOTICE

The author(s) is (are) the only responsible for the printed material included in this paper.